Fast Algorithm and Electromagnetic Field Behavior of 3D Photonic Crystals

Tiexiang Li

Southeast University
Nanjing Center for Applied Mathematics

joint work with Wen-Wei Lin, Xing-Long Lyu, Jia-Wei Lin, Tung-Ming Huang, Xin Liang, Heng Tian

2024 Current Developments in Mathematics and Physics

Contents

Photonic Crystals -**Periodic lattice composed of dielectric material**

Peacock feathers

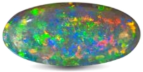

Opal

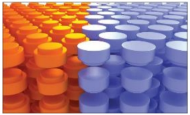

Hexagonal

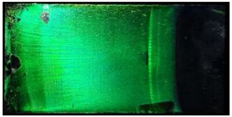

FCC

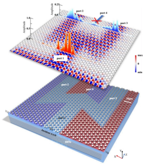

Fig. 3 High throughput SAW splitter based on the ETVS. (bottom) Schematic of a three-ports SAW splitter sample consists of the (blue shaded) VA, (red shaded) VB, and (unshaded) SM. In the experiment, planar SAWs are injected into the sample from Port#1 and captured from the other three ports. (upper) Calculated SAW out-of-plane displacement distributions and experimentally imaged SAW amplitude around all four ports. All SAWs are highly localized in routes that hold the same valley pseudospin, *i.e.*, the SAWs are output the sample only via Ports #2 and #3.

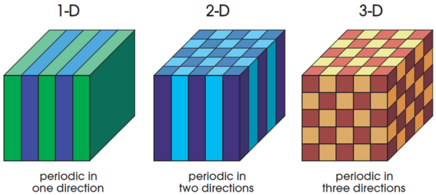

Contents

Maxwell Equations

Maxwell's equations for electromagnetic waves:

$$\nabla \times \boldsymbol{E} = \imath\omega \boldsymbol{B}, \qquad \nabla \times \boldsymbol{H} = -\imath\omega \boldsymbol{D}, \qquad \nabla \cdot \boldsymbol{B} = 0, \qquad \nabla \cdot \boldsymbol{D} = 0.$$

- **Dielectric material:** $\boldsymbol{D} = \varepsilon \boldsymbol{E}, \ \boldsymbol{B} = \mu \boldsymbol{H}$
- **Complex media:** $\boldsymbol{D} = \varepsilon \boldsymbol{E} + \xi \boldsymbol{H}, \ \boldsymbol{B} = \mu \boldsymbol{H} + \zeta \boldsymbol{E}$

where

- $\boldsymbol{E}$: electric field, $\boldsymbol{H}$: magnetic field
- $\boldsymbol{D}$: electric displacement field, $\boldsymbol{B}$: magnetic induction field
- ε: permittivity, μ: permeability
- ξ, ζ: magnetoelectric parameters (complex media)

3D Maxwell Eigenvalue Problems

Maxwell eigenvalue problems for 3D photonic crystals (MEPs):

$$\nabla \times \boldsymbol{E} = \imath\omega \boldsymbol{B}, \qquad \nabla \times \boldsymbol{H} = -\imath\omega \boldsymbol{D}, \qquad \nabla \cdot \boldsymbol{B} = 0, \qquad \nabla \cdot \boldsymbol{D} = 0.$$

- **Dielectric material:** $\boldsymbol{D} = \varepsilon \boldsymbol{E}, \; \boldsymbol{B} = \mu \boldsymbol{H}$

$$\dashrightarrow \nabla \times \mu^{-1} \nabla \times \boldsymbol{E} = \omega^2 \varepsilon \boldsymbol{E}, \qquad \nabla \cdot (\varepsilon \boldsymbol{E}) = 0;$$

- **Complex media:** $\boldsymbol{D} = \varepsilon \boldsymbol{E} + \xi \boldsymbol{H}, \; \boldsymbol{B} = \mu \boldsymbol{H} + \zeta \boldsymbol{E}$

$$\begin{bmatrix} -\nabla\times & 0 \\ 0 & \nabla\times \end{bmatrix} \begin{bmatrix} \boldsymbol{E} \\ \boldsymbol{H} \end{bmatrix} = \imath\omega \begin{bmatrix} \zeta & \mu \\ \varepsilon & \xi \end{bmatrix} \begin{bmatrix} \boldsymbol{E} \\ \boldsymbol{H} \end{bmatrix}, \quad \nabla \cdot \boldsymbol{B} = 0, \quad \nabla \cdot \boldsymbol{D} = 0.$$

Photonic Band Structure

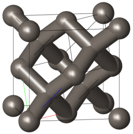

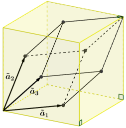

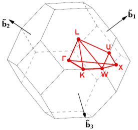

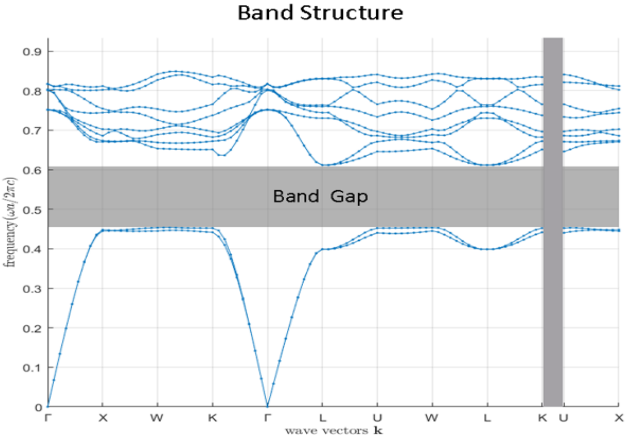

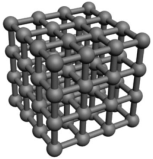

Photonic Bandgap: The frequency range where no electromagnetic eigenmode exists

Band Structure: A sequence of MEPs → finding several smallest positive eigenvalues

MEPs for Dielectric Material

Consider Maxwell's equations for 3D PhC:

$$\nabla \times \boldsymbol{E}(\mathbf{r}) = -\imath\omega \boldsymbol{B}(\mathbf{r}), \qquad \nabla \times \boldsymbol{H}(\mathbf{r}) = \imath\omega \boldsymbol{D}(\mathbf{r}), \qquad \nabla \cdot \boldsymbol{D}(\mathbf{r}) = 0, \qquad \nabla \cdot \boldsymbol{B}(\mathbf{r}) = 0.$$

- In combination with the linear constitutive relations

$$\boldsymbol{D}(\mathbf{r}) = \boldsymbol{\varepsilon}(\mathbf{r}) \cdot \boldsymbol{E}(\mathbf{r}), \quad \boldsymbol{B}(\mathbf{r}) = \boldsymbol{\mu}(\mathbf{r}) \cdot \boldsymbol{H}(\mathbf{r}),$$

  we obtain the MEPs:

$$\begin{bmatrix} -\nabla\times & 0 \\ 0 & \nabla\times \end{bmatrix} \begin{bmatrix} \boldsymbol{E} \\ \boldsymbol{H} \end{bmatrix} = \imath\omega \begin{bmatrix} 0 & \mu \\ \varepsilon & 0 \end{bmatrix} \begin{bmatrix} \boldsymbol{E} \\ \boldsymbol{H} \end{bmatrix}, \quad \nabla \cdot \boldsymbol{B} = 0, \quad \nabla \cdot \boldsymbol{D} = 0.$$

- The permittivity and permeability tensors $\boldsymbol{\varepsilon}$ and $\boldsymbol{\mu}$ are 3D periodic functions[1]

$$\boldsymbol{\varepsilon}(\mathbf{r} + \mathbf{a}_\ell) = \boldsymbol{\varepsilon}(\mathbf{r}), \quad \boldsymbol{\mu}(\mathbf{r} + \mathbf{a}_\ell) = \boldsymbol{\mu}(\mathbf{r}), \quad \ell = 1, 2, 3.$$

[1] For isotropic PhCs, $\boldsymbol{\mu} = 1$ and $\boldsymbol{\varepsilon}$ is just a scalar function; for anisotropic PhCs, $\boldsymbol{\mu}$ and $\boldsymbol{\varepsilon}$ are 3×3 Hermitian positive definite (HPD) tensors.

Quasi-Periodic Boundary Conditions

- **Bloch's Theorem:** On a given crystal lattice, eigenfields $\boldsymbol{E}$ as well as $\boldsymbol{H}$, $\boldsymbol{D}$ and $\boldsymbol{B}$ satisfy the quasi-periodic conditions

$$\boldsymbol{F}(\mathbf{r} + \mathbf{a}_\ell) = e^{\imath 2\pi \mathbf{k}\cdot\mathbf{a}_\ell} \boldsymbol{F}(\mathbf{r}), \quad \ell = 1, 2, 3,$$

where $\boldsymbol{F} = \boldsymbol{E}, \ \boldsymbol{H}, \ \boldsymbol{D}, \ \boldsymbol{B}, \ \mathbf{k}$ is Bloch wave vector in the first Brillouin zone $\mathcal{B}$, $\mathbf{a}_1, \ \mathbf{a}_2, \ \mathbf{a}_3$ are the lattice translation vectors.

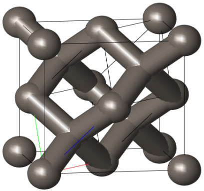

(a) FCC physical cell

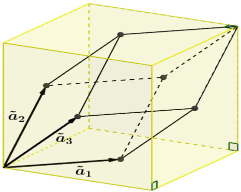

(b) Primitive cell Ω

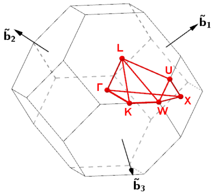

(c) First Brillouin zone $\mathcal{B}$

Figure: Illustration of the 3D quasi-periodic BCs

Lattice Translation Vectors $[\mathbf{a}_1, \mathbf{a}_2, \mathbf{a}_3]$

- There are 14 Bravais lattices, and they belong to 7 lattice systems.
- Each lattice has its associated lattice vectors.

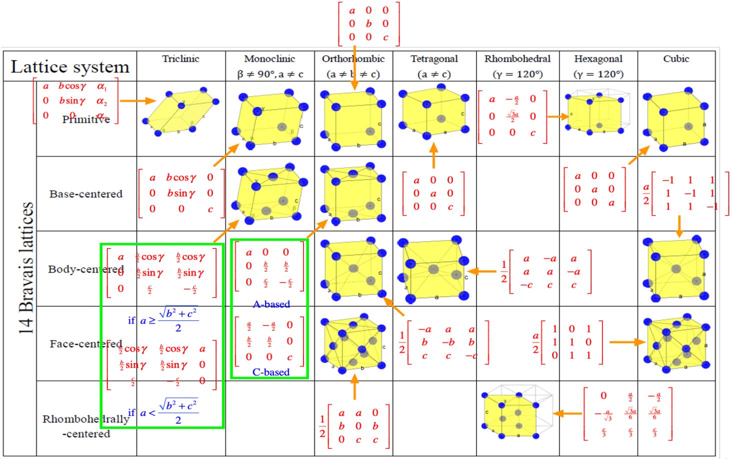

Governing Equations for 3D PhCs

Goal: Develop a uniform framework for anisotropic 3D PhCs with various Bravais lattices to find several the smallest positive eigenvalues ω and the corresponding eigenfields $\boldsymbol{E}$ and $\boldsymbol{H}$ of MEPs

$$\begin{bmatrix} -\nabla\times & 0 \\ 0 & \nabla\times \end{bmatrix} \begin{bmatrix} \boldsymbol{E} \\ \boldsymbol{H} \end{bmatrix} = \imath\omega \begin{bmatrix} 0 & \mu \\ \varepsilon & 0 \end{bmatrix} \begin{bmatrix} \boldsymbol{E} \\ \boldsymbol{H} \end{bmatrix}, \quad \nabla\cdot(\varepsilon\boldsymbol{E}) = 0, \quad \nabla\cdot(\mu\boldsymbol{D}) = 0, \tag{1}$$

with quasi-periodic conditions (**QQQ BCs**)

$$\boldsymbol{D}(\mathbf{r}+\mathbf{a}_\ell) = e^{\imath 2\pi \mathbf{k}\cdot\mathbf{a}_\ell}\boldsymbol{D}(\mathbf{r}), \boldsymbol{E}(\mathbf{r}+\mathbf{a}_\ell) = e^{\imath 2\pi \mathbf{k}\cdot\mathbf{a}_\ell}\boldsymbol{E}(\mathbf{r}), \ \ell = 1, 2, 3.$$

- Develop the Fast Algorithm for Maxwell Equations, **FAME**, with GPU accelerator to propose a high-performance computing package.

Contents

Oblique Coordinate Systems

- Given Bravais lattice vectors $[\mathbf{a}_1,\ \mathbf{a}_2,\ \mathbf{a}_3]$.
- Define reciprocal lattice vectors $\{\mathbf{a}^\ell\}_{\ell=1}^3$ such that

$$\mathbf{a}_i \cdot \mathbf{a}^j = \delta_i^j \equiv \begin{cases} 1, & i = j \\ 0, & i \neq j \end{cases} \quad i, j = 1, 2, 3.$$

- $\{\mathbf{a}_\ell\}_{\ell=1}^3$: the covariant basis, and $\{\mathbf{a}^\ell\}_{\ell=1}^3$: the contravariant basis.

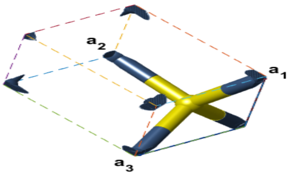

(a) FCC with lattice vectors $\{\mathbf{a}_\ell\}_{\ell=1}^3$.

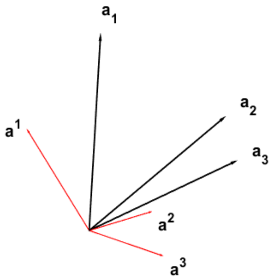

(b) Lattice and reciprocal lattice bases.

- Any position vector $\mathbf{r}$ and wave vector $\mathbf{k}$ can be written as

$$\mathbf{r} = r^1\mathbf{a}_1 + r^2\mathbf{a}_2 + r^3\mathbf{a}_3, \quad \mathbf{k} = k_1\mathbf{a}^1 + k_2\mathbf{a}^2 + k_3\mathbf{a}^3,$$

where $r^\ell = \mathbf{r} \cdot \mathbf{a}^\ell$ and $k_\ell = \mathbf{k} \cdot \mathbf{a}_\ell,\ \ell = 1, 2, 3$.

- The volume of primitive cell Ω satisfies

$$|\Omega| = \mathbf{a}_1 \cdot (\mathbf{a}_2 \times \mathbf{a}_3).$$

- The gradient operator ∇ and curl operator $\nabla\times$ can be represented as

$$\nabla \times \boldsymbol{F} = \mathbf{a}^i \times \left(\frac{\partial(\boldsymbol{F} \cdot \mathbf{a}_j)}{\partial r^i}\mathbf{a}^j\right) = \frac{1}{|\Omega|}\sum_{\ell,i,j=1}^{3} \epsilon^{\ell ij}\frac{\partial(\boldsymbol{F} \cdot \mathbf{a}_j)}{\partial r^i}\mathbf{a}_\ell,$$

$$\nabla \cdot \boldsymbol{F} = \sum_{\ell=1}^{3} \frac{\partial(\boldsymbol{F} \cdot \mathbf{a}^\ell)}{\partial r^\ell},$$

where $\boldsymbol{F} = \boldsymbol{E},\ \boldsymbol{H},\ \boldsymbol{D},\ \boldsymbol{B}$. ϵ: Levi-Civita symbol, $\epsilon^{\ell ij} = 1((\ell, i, j)$ are even permutation); $-1((\ell, i, j)$ are odd permutation); $0(\ell,\ i$ and j have two same indices).

Representations of $\nabla\times$ and $\nabla\cdot$ in oblique coordinates

In oblique coordinate system $\{\mathbf{a}_\ell\}_{\ell=1}^3$, Maxwell's equations have the forms

$$\frac{1}{|\Omega|}\sum_{i,j=1}^{3}\epsilon^{\ell ij}\frac{\partial E_j}{\partial r^i} = \imath\omega B^\ell, \quad \frac{1}{|\Omega|}\sum_{i,j=1}^{3}\epsilon^{\ell ij}\frac{\partial H_j}{\partial r^i} = -\imath\omega D^\ell, \quad \sum_{\ell=1}^{3}\frac{\partial D^\ell}{\partial r^\ell} = \sum_{\ell=1}^{3}\frac{\partial B^\ell}{\partial r^\ell} = 0, \quad \ell = 1,2,3,$$

where the components of $\boldsymbol{D}$ and $\boldsymbol{B}$ on $\{\mathbf{a}_\ell\}_{\ell=1}^3$ as well as, $\boldsymbol{E}$ and $\boldsymbol{H}$ on $\{\mathbf{a}^\ell\}_{\ell=1}^3$ are given by

$$\boldsymbol{D} = \sum_{\ell=1}^{3}(\boldsymbol{D}\cdot\mathbf{a}^\ell)\mathbf{a}_\ell = \sum_{\ell=1}^{3}D^\ell\mathbf{a}_\ell, \quad \boldsymbol{B} = \sum_{\ell=1}^{3}B^\ell\mathbf{a}_\ell,$$

$$\boldsymbol{E} = \sum_{\ell=1}^{3}(\boldsymbol{E}\cdot\mathbf{a}_\ell)\mathbf{a}^\ell = \sum_{\ell=1}^{3}E_\ell\mathbf{a}^\ell, \quad \boldsymbol{H} = \sum_{\ell=1}^{3}H_\ell\mathbf{a}^\ell.$$

Representations of constitutive relations

Write $A = [\mathbf{a}_1, \mathbf{a}_2, \mathbf{a}_3]$ and $A^{-1} = [\mathbf{a}^1, \mathbf{a}^2, \mathbf{a}^3]^\top$, for the constitutive relations

$$\boldsymbol{E}(\mathbf{r}) = \varepsilon^{-1}(\mathbf{r})\boldsymbol{D}(\mathbf{r}), \quad \boldsymbol{H}(\mathbf{r}) = \boldsymbol{\mu}^{-1}(\mathbf{r})\boldsymbol{B}(\mathbf{r}),$$

we have the matrix-vector form

$$\begin{bmatrix} E_1 \\ E_2 \\ E_3 \end{bmatrix} = A^\top \boldsymbol{E}(\mathbf{r}) = A^\top \varepsilon^{-1}(\mathbf{r}) A \cdot A^{-1} \boldsymbol{D}(\mathbf{r}) = \begin{bmatrix} [\varepsilon_{\text{cov}}^{-1}]_{11} & [\varepsilon_{\text{cov}}^{-1}]_{12} & [\varepsilon_{\text{cov}}^{-1}]_{13} \\ [\varepsilon_{\text{cov}}^{-1}]_{21} & [\varepsilon_{\text{cov}}^{-1}]_{22} & [\varepsilon_{\text{cov}}^{-1}]_{23} \\ [\varepsilon_{\text{cov}}^{-1}]_{31} & [\varepsilon_{\text{cov}}^{-1}]_{32} & [\varepsilon_{\text{cov}}^{-1}]_{33} \end{bmatrix} \begin{bmatrix} D^1 \\ D^2 \\ D^3 \end{bmatrix},$$

$$\begin{bmatrix} H_1 \\ H_2 \\ H_3 \end{bmatrix} = \begin{bmatrix} [\boldsymbol{\mu}_{\text{cov}}^{-1}]_{11} & [\boldsymbol{\mu}_{\text{cov}}^{-1}]_{12} & [\boldsymbol{\mu}_{\text{cov}}^{-1}]_{13} \\ [\boldsymbol{\mu}_{\text{cov}}^{-1}]_{21} & [\boldsymbol{\mu}_{\text{cov}}^{-1}]_{22} & [\boldsymbol{\mu}_{\text{cov}}^{-1}]_{23} \\ [\boldsymbol{\mu}_{\text{cov}}^{-1}]_{31} & [\boldsymbol{\mu}_{\text{cov}}^{-1}]_{32} & [\boldsymbol{\mu}_{\text{cov}}^{-1}]_{33} \end{bmatrix} \begin{bmatrix} B^1 \\ B^2 \\ B^3 \end{bmatrix},$$

where

$$[\varepsilon_{\text{cov}}^{-1}]_{pq}(\mathbf{r}) = \mathbf{a}_p \cdot \varepsilon^{-1}(\mathbf{r}) \cdot \mathbf{a}_q, \; [\boldsymbol{\mu}_{\text{cov}}^{-1}]_{pq}(\mathbf{r}) = \mathbf{a}_p \cdot \boldsymbol{\mu}^{-1}(\mathbf{r}) \cdot \mathbf{a}_q, \; p, q = 1, 2, 3.$$

- ε^{-1} and $\boldsymbol{\mu}^{-1}$, hence $[\varepsilon_{\text{cov}}^{-1}]$ and $[\boldsymbol{\mu}_{\text{cov}}^{-1}]$, are 3-by-3 HPD matrices.

Representations of boundary conditions

For quasi-periodic boundary conditions

$$\boldsymbol{E}(\mathbf{r}+\mathbf{a}_\ell) = e^{\imath 2\pi \mathbf{k}\cdot\mathbf{a}_\ell}\boldsymbol{E}(\mathbf{r}), \quad \boldsymbol{H}(\mathbf{r}+\mathbf{a}_\ell) = e^{\imath 2\pi \mathbf{k}\cdot\mathbf{a}_\ell}\boldsymbol{H}(\mathbf{r}),$$

they are particularly simple as

$$E_q(r^1+\delta_\ell^1, r^2+\delta_\ell^2, r^3+\delta_\ell^3) = \exp(\imath 2\pi \mathbf{k}\cdot\mathbf{a}_\ell) E_q(r^1, r^2, r^3), \quad q = 1, 2, 3.$$

The same goes for $\boldsymbol{H}$.

Yee's scheme in oblique coordinates

$$i \in \mathbb{N}_1 := \{0, 1, \ldots, n_1 - 1\}, \quad j \in \mathbb{N}_2 := \{0, 1, \ldots, n_2 - 1\}, \quad k \in \mathbb{N}_3 := \{0, 1, \ldots, n_3 - 1\}.$$

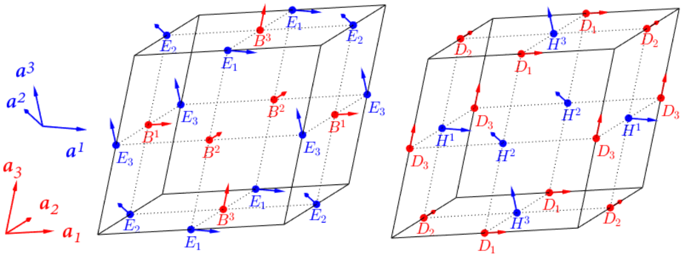

Figure: Setting up of $\boldsymbol{E}$ and $\boldsymbol{B}$, $\boldsymbol{H}$ and $\boldsymbol{D}$ by Yee's scheme in oblique coordinates.

- Sampling points of $\{D^\ell\}_{\ell=1}^3$ and $\{E_\ell\}_{\ell=1}^3$ are the same,
- Sampling points of $\{B^\ell\}_{\ell=1}^3$ and $\{H_\ell\}_{\ell=1}^3$ are the same.

FD Discretization of $\nabla\times$ and $\nabla\cdot$ with QQQ BCs

Combining with Bloch conditions, the first-order central finite difference (FD) discretization of all the partial derivatives can be formulated as:

- Matrix-vector form of $\partial E_q/\partial r^\ell, q, \ell = 1,2,3, q \neq \ell$,

$$\partial E_q/\partial r^1 \Longrightarrow C_1\mathbf{e}_q \equiv n_1(I_{n_3} \otimes I_{n_2} \otimes K_{n_1}(\mathbf{k}\cdot\mathbf{a}_1) - I_n)\mathbf{e}_q,\ \ q = 2,3,$$
$$\partial E_q/\partial r^2 \Longrightarrow C_2\mathbf{e}_q \equiv n_2(I_{n_3} \otimes K_{n_2}(\mathbf{k}\cdot\mathbf{a}_2) \otimes I_{n_1} - I_n)\mathbf{e}_q,\ \ q = 1,3,$$
$$\partial E_q/\partial r^3 \Longrightarrow C_3\mathbf{e}_q \equiv n_3(K_{n_3}(\mathbf{k}\cdot\mathbf{a}_3) \otimes I_{n_2} \otimes I_{n_1} - I_n)\mathbf{e}_q,\ \ q = 1,2,$$

  where $n = n_1n_2n_3$, $\mathbf{e}_q := \mathrm{vec}(\{E_q(i,j,k)\}_{i\in\mathbb{N}_1, j\in\mathbb{N}_2, k\in\mathbb{N}_3}), q = 1,2,3,$

$$K_m(\theta) := \begin{bmatrix} 0 & I_{m-1} \\ e^{\imath 2\pi\theta} & 0 \end{bmatrix} \in \mathbb{C}^{m\times m},\ \ \theta\in\mathbb{R},\ \ m\in\mathbb{N} = \{n_1, n_2, n_3\}.$$

- $K_m(\theta)$ is unitary with the elegant decomposition

$$K_m(\theta) = \exp(\imath 2\pi\theta/m) W_m(\theta)^* F_m^* W_m(1) F_m W_m(\theta),$$

  with unitary $W_m(\theta) = \mathbf{diag}(\exp(\imath 2\pi\theta[0\colon m-1]/m))$, and F_m is the discrete Fourier transform matrix (DFT) .

- Similarly $\partial H_q/\partial r^1 \Rightarrow -C_1^*\mathbf{h}_q,\quad \partial H_q/\partial r^2 \Rightarrow -C_2^*\mathbf{h}_q,\quad \partial H_q/\partial r^3 \Rightarrow -C_3^*\mathbf{h}_q.$

Then the discretizations for

$$-\nabla \times \boldsymbol{E} = \imath\omega \boldsymbol{B}, \quad \nabla \times \boldsymbol{H} = \imath\omega \boldsymbol{D}$$

can be obtained as:

$$-\imath\omega \mathbf{b} = \mathcal{C}\mathbf{e}, \ \imath\omega \mathbf{d} = \mathcal{C}^* \mathbf{h} \ \text{ with } \ \mathcal{C} := \frac{1}{|\Omega|} \begin{bmatrix} 0 & -C_3 & C_2 \\ C_3 & 0 & -C_1 \\ -C_2 & C_1 & 0 \end{bmatrix},$$

- satisfying

$$\boxed{C_\ell T = T\left(\Lambda_\ell - I_n\right) n_\ell, \quad C_\ell^* T = T\left(\Lambda_\ell^* - I_n\right) n_\ell, \quad \ell = 1, 2, 3}$$

$$\Lambda_1 = I_{n_3} \otimes I_{n_2} \otimes \left(\xi_1 W_{n_1}(1)\right), \quad \Lambda_2 = I_{n_3} \otimes \left(\xi_2 W_{n_2}(1)\right) \otimes I_{n_1}, \quad \Lambda_3 = \left(\xi_3 W_{n_3}(1)\right) \otimes I_{n_2} \otimes I_{n_1},$$

$$T = \left(W_{n_3}(\mathbf{k}\cdot\mathbf{a}_3) \otimes W_{n_2}(\mathbf{k}\cdot\mathbf{a}_2) \otimes W_{n_1}(\mathbf{k}\cdot\mathbf{a}_1)\right)\left(F_{n_3}^* \otimes F_{n_2}^* \otimes F_{n_1}^*\right), \quad \xi_\ell = \exp\left(\imath 2\pi \mathbf{k}\cdot\mathbf{a}_\ell / n_\ell\right).$$

- $\{C_p, C_p^*\}_{p=1}^3$ is a set of commutative normal matrices with $K_m^*(\theta) K_m(\theta) = I_m$.

$$T\mathbf{q} = (W_{n_3}(\mathbf{k}\cdot\mathbf{a}_3) \otimes W_{n_2}(\mathbf{k}\cdot\mathbf{a}_2) \otimes W_{n_1}(\mathbf{k}\cdot\mathbf{a}_1))(F_{n_3} \otimes F_{n_2} \otimes F_{n_1})\mathbf{q} \longleftarrow \textbf{3D FFT}$$

$$T^*\mathbf{p} = (F_{n_3}^* \otimes F_{n_2}^* \otimes F_{n_1}^*)(W_{n_3}^*(\mathbf{k}\cdot\mathbf{a}_3) \otimes W_{n_2}^*(\mathbf{k}\cdot\mathbf{a}_2) \otimes W_{n_1}^*(\mathbf{k}\cdot\mathbf{a}_1))\mathbf{p} \longleftarrow \textbf{3D IFFT}$$

$$C_\ell T = T(\Lambda_\ell - I_n)\, n_\ell, \quad C_\ell^* T = T(\Lambda_\ell^* - I_n)\, n_\ell, \ \ell = 1, 2, 3$$

- $\mathcal{C} N_c = 0$, $N_c = [C_1^\top, C_2^\top, C_3^\top]$.
- $\mathcal{C}$ has a singular value decomposition (**SVD**)

$$\mathcal{C} = P \mathrm{diag}(\Lambda_q^{1/2}, \Lambda_q^{1/2}, 0) Q^* = P_r \Sigma_r Q_r^*, \quad \Sigma_r = \mathrm{diag}(\Lambda_q^{1/2}, \Lambda_q^{1/2})$$

with $\Lambda_q = \Lambda_1^* \Lambda_1 + \Lambda_2^* \Lambda_2 + \Lambda_3^* \Lambda_3$, and

$$Q_r = (I_3 \otimes T) \begin{bmatrix} \ddots & \ddots \\ \ddots & \ddots \\ \ddots & \ddots \end{bmatrix}$$

Range space

Null space

$$Q = [Q_r | Q_0] \equiv (I_3 \otimes T) \left[\ \Pi_1\, \Pi_2 \,|\, \Pi_0\ \right] \equiv (I_3 \otimes T) \begin{bmatrix} \ddots & \ddots & \ddots \\ \ddots & \ddots & \ddots \\ \ddots & \ddots & \ddots \end{bmatrix},$$

$$P = [P_r | P_0] = (I_3 \otimes T) \left[\ -\bar{\Pi}_2\, \bar{\Pi}_1 \,|\, \bar{\Pi}_0\ \right],$$

where $Q_r, P_r \in \mathbb{C}^{3n \times 2n}$ are unitary and $\Pi_{i,j} \in \mathbb{C}^{n \times n}$ are diagonal.

★ $\mathcal{C}$ has the special structure which can easily be treated with the 3D FFT and 3D IFFT to accelerate the numerical simulation.

Discretization of constitutive relations

For the constitutive relations in oblique coordinate system

$$\left[E_1, E_2, E_3\right]^\top = [\varepsilon_{\text{cov}}^{-1}]\left[D^1, D^2, D^3\right]^\top, \ \left[H_1, H_2, H_3\right]^\top = [\boldsymbol{\mu}_{\text{cov}}^{-1}]\left[B^1, B^2, B^3\right]^\top,$$

with

$$[\varepsilon_{\text{cov}}^{-1}]_{pq}(\mathbf{r}) = \mathbf{a}_p \cdot \varepsilon^{-1}(\mathbf{r}) \cdot \mathbf{a}_q, \ [\boldsymbol{\mu}_{\text{cov}}^{-1}]_{pq}(\mathbf{r}) = \mathbf{a}_p \cdot \boldsymbol{\mu}^{-1}(\mathbf{r}) \cdot \mathbf{a}_q, \ p, q = 1, 2, 3,$$

we denote

$$[\varepsilon_{\text{cov}}^{-1}]_{pq,ijk} = [\varepsilon_{\text{cov}}^{-1}]_{pq}(i/n_1, j/n_2, k/n_3), \ [\boldsymbol{\mu}_{\text{cov}}^{-1}]_{pq,ijk} = [\boldsymbol{\mu}_{\text{cov}}^{-1}]_{pq}\left(\hat{i}/n_1, \hat{j}/n_2, \hat{k}/n_3\right), \quad i \in \mathbb{N}_1, j \in \mathbb{N}_2, k \in \mathbb{N}_3, \ p, q = 1, 2, 3.$$

Define an interpolation operator on $\boldsymbol{E}$ and $\boldsymbol{H}$, as

$$\begin{aligned} E_{1,ijk} \approx & \frac{1}{2}([\varepsilon_{\text{cov}}^{-1}]_{11,ijk} + [\varepsilon_{\text{cov}}^{-1}]_{11,(i+1)jk}) D^1_{ijk} + \\ & \frac{1}{2}\left([\varepsilon_{\text{cov}}^{-1}]_{12,ijk} \frac{1}{2}\left(D^2_{ijk} + D^2_{i(j-1)k}\right) + [\varepsilon_{\text{cov}}^{-1}]_{12,(i+1)jk} \frac{1}{2}\left(D^2_{(i+1)jk} + D^2_{(i+1)(j-1)k}\right)\right) + \\ & \frac{1}{2}\left([\varepsilon_{\text{cov}}^{-1}]_{13,ijk} \frac{1}{2}\left(D^3_{ijk} + D^3_{ij(k-1)}\right) + [\varepsilon_{\text{cov}}^{-1}]_{13,(i+1)jk} \frac{1}{2}\left(D^3_{(i+1)jk} + D^3_{(i+1)j(k-1)}\right)\right). \end{aligned}$$

Discretization of constitutive relations

Then for the constitutive relations $\boldsymbol{E}(\mathbf{r}) = \boldsymbol{\varepsilon}^{-1}(\mathbf{r})\boldsymbol{D}(\mathbf{r})$, $\boldsymbol{H}(\mathbf{r}) = \boldsymbol{\mu}^{-1}(\mathbf{r})\boldsymbol{B}(\mathbf{r})$, we have the discretized form

$$\mathbf{e} = \mathcal{N}_{\text{int}}\mathbf{d} = \left(\left(\mathcal{K} + I_{3n}\right)\left(\mathcal{N} - \mathcal{N}_d\right)\left(\mathcal{K}^* + I_{3n}\right) + 2\mathcal{K}\mathcal{N}_d\mathcal{K}^* + 2\mathcal{N}_d \right)\mathbf{d}/4,$$
$$\mathbf{h} = \mathcal{M}_{\text{int}}\mathbf{b} = \left(\left(\mathcal{K}^* + I_{3n}\right)\left(\mathcal{M} - \mathcal{M}_d\right)\left(\mathcal{K} + I_{3n}\right) + 2\mathcal{K}^*\mathcal{M}_d\mathcal{K} + 2\mathcal{M}_d \right)\mathbf{b}/4,$$

where

$$\mathcal{K} = \left(I_n + C_1/n_1\right) \oplus \left(I_n + C_2/n_2\right) \oplus \left(I_n + C_3/n_3\right),$$
$$\mathcal{N}_d = \mathbf{diag}\left(N_{11}\right) \oplus \mathbf{diag}\left(N_{22}\right) \oplus \mathbf{diag}\left(N_{33}\right), \mathcal{M}_d = \mathbf{diag}\left(M_{11}\right) \oplus \mathbf{diag}\left(M_{22}\right) \oplus \mathbf{diag}\left(M_{33}\right),$$
$$\mathcal{N} = \begin{bmatrix} \mathbf{diag}(N_{11}) & \mathbf{diag}(N_{12}) & \mathbf{diag}(N_{13}) \\ \mathbf{diag}(N_{21}) & \mathbf{diag}(N_{22}) & \mathbf{diag}(N_{23}) \\ \mathbf{diag}(N_{31}) & \mathbf{diag}(N_{32}) & \mathbf{diag}(N_{33}) \end{bmatrix}, \quad \mathcal{M} = \begin{bmatrix} \mathbf{diag}(M_{11}) & \mathbf{diag}(M_{12}) & \mathbf{diag}(M_{13}) \\ \mathbf{diag}(M_{21}) & \mathbf{diag}(M_{22}) & \mathbf{diag}(M_{23}) \\ \mathbf{diag}(M_{31}) & \mathbf{diag}(M_{32}) & \mathbf{diag}(M_{33}) \end{bmatrix},$$
$$N_{pq} = \text{vec}([\varepsilon_{\text{cov}}^{-1}]_{pq}(i,j,k)), \quad M_{pq} = \text{vec}([\mu_{\text{cov}}^{-1}]_{pq}(i,j,k)), \quad i \in \mathbb{N}_1, \quad j \in \mathbb{N}_2, \quad k \in \mathbb{N}_3, \quad p, \quad q = 1, 2, 3.$$

- Both $\mathcal{N}_{\text{int}}$ and $\mathcal{M}_{\text{int}}$ are Hermite positive definite (HPD).
- Both $\mathcal{K}\mathcal{N}_d\mathcal{K}^*$ and $\mathcal{K}^*\mathcal{M}_d\mathcal{K}$ are diagonal matrices.

Discretized MEP with QQQ BCs $\Leftrightarrow$ A Null-Space Free GEP

Utilizing above discretization scheme, MEP can be discretized into a GEP

$$\begin{bmatrix} -\nabla\times & 0 \\ 0 & \nabla\times \end{bmatrix} \begin{bmatrix} \boldsymbol{E} \\ \boldsymbol{H} \end{bmatrix} = \imath\omega \begin{bmatrix} 0 & \mu \\ \varepsilon & 0 \end{bmatrix} \begin{bmatrix} \boldsymbol{E} \\ \boldsymbol{H} \end{bmatrix} \Longrightarrow \begin{bmatrix} -\mathcal{C} & 0 \\ 0 & \mathcal{C}^* \end{bmatrix} \begin{bmatrix} \mathbf{e} \\ \mathbf{h} \end{bmatrix} = \imath\omega \begin{bmatrix} 0 & \mathcal{M}_{\text{int}}^{-1} \\ \mathcal{N}_{\text{int}}^{-1} & 0 \end{bmatrix} \begin{bmatrix} \mathbf{e} \\ \mathbf{h} \end{bmatrix}.$$

- With the SVD of $\mathcal{C} = P_r \Sigma_r Q_r^*$, the above GEP can be transformed into a null-space free GEP:

$$\begin{bmatrix} -\Sigma_r & 0 \\ 0 & \Sigma_r \end{bmatrix} \begin{bmatrix} \mathbf{e}^r \\ \mathbf{h}^r \end{bmatrix} = \imath\omega \begin{bmatrix} 0 & \mathcal{M}_{\text{int,r}}^{-1} \\ \mathcal{N}_{\text{int,r}}^{-1} & 0 \end{bmatrix} \begin{bmatrix} \mathbf{e}^r \\ \mathbf{h}^r \end{bmatrix},$$

  or by replacing $\mathbf{e}^r$ with $(-\imath\omega^{-1})\mathcal{N}_{\text{int,r}}^{-1}\Sigma_r\mathbf{h}^r$ to obtain

$$\boxed{\mathcal{A}_r\mathbf{h}^r \equiv \Sigma_r \mathcal{N}_{\text{int,r}} \Sigma_r \mathbf{h}^r = \omega^2 \mathcal{M}_{\text{int,r}}^{-1} \mathbf{h}^r,}$$

  where $\mathcal{N}_{\text{int,r}} := P_r^* \mathcal{N}_{\text{int}}^{-1} P_r$ and $\mathcal{M}_{\text{int,r}} := Q_r^* \mathcal{M}_{\text{int}}^{-1} Q_r$.

- $\mathcal{M}_{\text{int}} \equiv I$ and $\mathcal{N}_{\text{int}} \succ 0$ (i.e. the permeability $\mu \equiv 1$ and the permittivity $\varepsilon(\mathbf{r}) \succ 0$ for all $\mathbf{r} \in \Omega$).

MEPs for 3D PhC with Quasi-periodic BCs

For GEP from 3D anisotropic photonic crystal with QQQ BCs

$$\begin{bmatrix} -\mathcal{C} & 0 \\ 0 & \mathcal{C}^* \end{bmatrix} \begin{bmatrix} \mathbf{e} \\ \mathbf{h} \end{bmatrix} = \imath\omega \begin{bmatrix} 0 & \mathcal{M}_{\text{int}}^{-1} \\ \mathcal{N}_{\text{int}}^{-1} & 0 \end{bmatrix} \begin{bmatrix} \mathbf{e} \\ \mathbf{h} \end{bmatrix}$$

$$\Rightarrow \mathcal{A}_r \mathbf{h}^r \equiv \Sigma_r \mathcal{N}_{\text{int},r} \Sigma_r \mathbf{h}^r = \omega^2 \mathcal{M}_{\text{int},r}^{-1} \mathbf{h}^r \text{ with } \mathbf{h}^r \in \mathbb{C}^{2N_s+N_c}$$

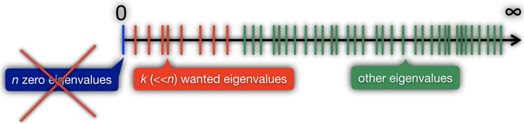

- **Numerical Challenges:**

✓ $\mathcal{C}$: singular, non-Hermitian;

✓ There exist zero eigenvalues with approximately one third of the number of coefficient matrices;

✓ Need a few smallest positive eigenvalues;

✓ The matrix dimension is very **Large!** Especially for supercell structure.

★ **Goal: compute several smallest positive eigenvalues of $\mathcal{A}_r \mathbf{x} = \lambda \mathbf{x}$.**

Eigensolver for MEPs with Quasi-periodic BCs

For SEP from 3D anisotropic photonic crystal

$$\begin{bmatrix} -\mathcal{C} & 0 \\ 0 & \mathcal{C}^* \end{bmatrix} \begin{bmatrix} \mathbf{e} \\ \mathbf{h} \end{bmatrix} = \imath\omega \begin{bmatrix} 0 & \mathcal{M}_{\text{int}}^{-1} \\ \mathcal{N}_{\text{int}}^{-1} & 0 \end{bmatrix} \begin{bmatrix} \mathbf{e} \\ \mathbf{h} \end{bmatrix}$$

$$\Rightarrow \mathcal{A}_r \mathbf{h}^r \equiv \Sigma_r \mathcal{N}_{\text{int},r} \Sigma_r \mathbf{h}^r = \omega^2 \mathcal{M}_{\text{int},r}^{-1} \mathbf{h}^r \text{ with } \mathbf{h}^r \in \mathbb{C}^{2N_s+N_c}.$$

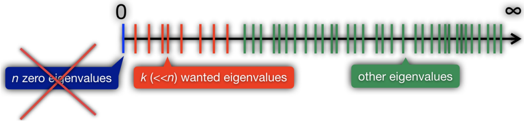

- **null-space free + FFT:**

✓ $\mathcal{A}_r$: nonsingular, Hermitian positive definite ←-- **null-space free transformation**

✓ There exist no zero eigenvalues in $\mathcal{A}_r$ ←-- **null-space free GEP**

✓ Need a few of smallest positive eigenvalues ←-- **inverse Lanczos + CG!**

✓ Dimension is very **Large!** ←-- **3D FFT, Highly suitable for parallel processing!**

Contents

MEPs for Chiral Media

Let relative permeability $\mu := 1$. Consider the electromagnetic fields in bi-isotropic chiral media

$$\begin{bmatrix} 0 & -\imath\nabla\times \\ \imath\nabla\times & 0 \end{bmatrix} \begin{bmatrix} \boldsymbol{H} \\ \boldsymbol{E} \end{bmatrix} = \omega \begin{bmatrix} \mu & \zeta \\ \xi & \varepsilon \end{bmatrix} \begin{bmatrix} \boldsymbol{H} \\ \boldsymbol{E} \end{bmatrix}. \tag{3}$$

where ζ and ξ satisfying

$$\varepsilon(\mathbf{x}) = \begin{cases} \varepsilon_i, & \mathbf{x} \in \text{material}, \\ \varepsilon_o, & \text{otherwise}, \end{cases} \zeta(\mathbf{x}) = \begin{cases} -\imath\gamma, & \mathbf{x} \in \text{material}, \\ 0, & \text{otherwise}, \end{cases} \xi(\mathbf{x}) = \begin{cases} \imath\gamma, & \mathbf{x} \in \text{material}, \\ 0, & \text{otherwise}, \end{cases}$$

and $\varepsilon_i > 0, \varepsilon_o > 0, \gamma \geq 0$.

- **Goal:** Find the smallest positive eigenvalues and their corresponding eigenvectors.

Discretization of MEPs

- By Yee's scheme, we obtain a generalized eigenvalue problem (GEP)

$$\begin{bmatrix} 0 & -\imath \boxed{\nabla\times} \\ \imath\nabla\times & 0 \end{bmatrix} \begin{bmatrix} \boldsymbol{H} \\ \boldsymbol{E} \end{bmatrix} = \omega \begin{bmatrix} \mu & \zeta \\ \xi & \varepsilon \end{bmatrix} \begin{bmatrix} \boldsymbol{H} \\ \boldsymbol{E} \end{bmatrix} \Longrightarrow$$

$$\begin{bmatrix} 0 & -\imath \boxed{\mathcal{C}} \\ \imath\mathcal{C}^* & 0 \end{bmatrix} \begin{bmatrix} \mathbf{h} \\ \mathbf{e} \end{bmatrix} = \omega \begin{bmatrix} \mu_d & \zeta_d \\ \xi_d & \varepsilon_d \end{bmatrix} \begin{bmatrix} \mathbf{h} \\ \mathbf{e} \end{bmatrix} \equiv A\mathbf{x} = \omega B(\gamma)\mathbf{x}$$

  where $\mathbf{h}, \mathbf{e} \in \mathbb{C}^{3n}$.

- $\mu_d, \varepsilon_d, \xi_d, \zeta_d \in \mathbb{C}^{3n\times 3n}$ are diagonal with the following structures

$$\mu_d = I_{3n}, \qquad \varepsilon_d = \varepsilon_0 \boldsymbol{I}^{(0)} + \varepsilon_i \boldsymbol{I}^{(i)},$$

$$\zeta_d = -\imath\gamma \boldsymbol{I}^{(i)}, \qquad \xi_d = \imath\gamma \boldsymbol{I}^{(i)},$$

  where ε_i, ε_0 are the permittivities inside and outside the medium, $\gamma > 0$ is the chirality, $\boldsymbol{I}^{(i)} \in \mathbb{R}^{3n\times 3n}$ denotes the diagonal matrix with the j-th diagonal entry being 1 for the corresponding j-th discrete point inside the material and zero otherwise, $\boldsymbol{I}^{(0)} = I_{3n} - \boldsymbol{I}^{(i)}$.

★ **Goal: compute several smallest positive eigenvalues of $A\mathbf{x} = \omega B(\gamma)\mathbf{x}$.**

Study the Electromagnetic Field Behavior Theoretically

With the assumption $\mu = 1$ we can rewrite

$$\begin{bmatrix} I_{3n} & 0 \\ \xi_d \mu_d^{-1} & I_{3n} \end{bmatrix} \twoheadrightarrow (A, B(\gamma)) \equiv \left(\begin{bmatrix} 0 & -\imath\mathcal{C} \\ \imath\mathcal{C}^* & 0 \end{bmatrix}, \begin{bmatrix} \mu_d & \zeta_d \\ \xi_d & \varepsilon_d \end{bmatrix} \right) \twoheadleftarrow \begin{bmatrix} I_{3n} & \mu_d^{-1}\zeta_d \\ 0 & I_{3n} \end{bmatrix}$$

as

$$\left(\begin{bmatrix} 0 & -\imath\mathcal{C} \\ \imath\mathcal{C}^* & -\gamma[I^{(i)}\mathcal{C} + \mathcal{C}^* I^{(i)}] \end{bmatrix}, \begin{bmatrix} I_{3n} & 0 \\ 0 & \varepsilon_0 \mathbf{I}^{(0)} + (\varepsilon_{\mathbf{i}} - \gamma^2)\mathbf{I}^{(\mathbf{i})} \end{bmatrix} \right) \equiv (A_\gamma, B_\gamma)$$

A_γ is Hermitian, singular, indefinite

we call $\gamma^* \equiv \sqrt{\varepsilon_i}$ as critical chirality

- when $\gamma < \gamma^*$, (A_γ, B_γ) with $B_\gamma > 0$ being positive definite has all real eigenvalues
- when $\gamma > \gamma^*$, B_γ is indefinite and (A_γ, B_γ) has complex eigenvalues
- when $\gamma = \gamma^*$, $B_\gamma^* = \mathrm{diag}(I_{3n}, \varepsilon_0 I^{(0)})$ is semi-positive definite

$\Rightarrow$ (A_γ, B_γ) has infinite eigenvalues $\omega = \infty$

$\Rightarrow$ we can prove that there exist a lot of $\omega = \infty$ coming from 2×2 Jordan blocks!

- when $\gamma > \gamma^*$, B_γ is indefinite and (A_γ, B_γ) has complex eigenvalues
- when $\gamma = \gamma^*$, we can prove that (A_γ, B_γ) has 2×2 Jordan blocks at $\omega = \infty$

Furthermore, we can prove that:

- For $\gamma^+ = \gamma^* + \eta$ as $\eta \to 0^+$, $A_{\gamma^+} - \omega B_{\gamma^+}$ has at least one complex conjugate eigenvalue pairs $\omega_\pm(\gamma^+)$ with large imaginary part.
- At $\gamma = \gamma^+$, the electric field $\boldsymbol{E}(\mathbf{x}) \approx 0$ when $\mathbf{x}$ is outside the material.
- Increasing $\gamma^+ \to \gamma^0 \to \gamma^1 \Rightarrow \omega_\pm(\gamma) \in \mathbb{C} \to \omega_\pm(\gamma^1) \in \mathbb{R}$. Bifurcation happened at γ^0.
- $\omega_+(\gamma^1) > 0$ is the new smallest positive real eigenvalues.
- In this case, at $\gamma = \gamma^1$, the electric field $\boldsymbol{E}(\mathbf{x}) \approx 0$ when $\mathbf{x}$ is outside the material.

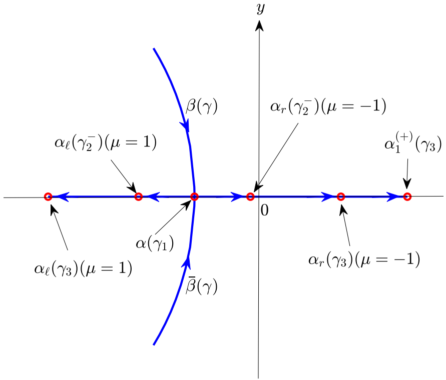

(a) Scenario of bifurcation

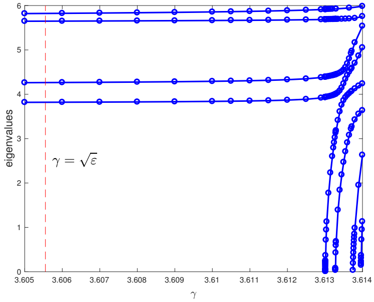

(b) Eigencurve-structure vs. γ

Figure: Conjugate eigenvalue pair and eigencurve-structure with $\gamma^* = \sqrt{13}$

Eigensolver for MEP for Chiral PhCs

- By Yee's scheme, we obtain a GEP for bi-isotropic chiral media (3)

$$\begin{bmatrix} 0 & -\imath \boxed{C} \\ \imath C^* & 0 \end{bmatrix} \begin{bmatrix} \mathbf{h} \\ \mathbf{e} \end{bmatrix} = \omega \begin{bmatrix} \mu_d & \zeta_d \\ \xi_d & \varepsilon_d \end{bmatrix} \begin{bmatrix} \mathbf{h} \\ \mathbf{e} \end{bmatrix} \equiv A\mathbf{x} = \omega B(\gamma)\mathbf{x} \text{ with } \mathbf{x} \in \mathbb{C}^{6n}$$

★ **Goal: compute several smallest positive eigenvalues of $A\mathbf{x} = \lambda B\mathbf{x}$.**

- **Numerical Challenges:**

✓ A: complex Hermitian, singular, maybe indefinite

✓ B: complex Hermitian, block sparse, maybe indefinite (depending on the magnetoelectric parameters)

✓ There exist $2n$ zero eigenvalues

✓ Need a few of smallest positive eigenvalues

✓ Dimension $3n$ or $6n$ is very **Large!** **($\geq 5,000,000$)**

Null Space Free Method $(6n \to 4n)$

Transform GEP into a null-space free standard eigenvalue problem with $\gamma \neq \gamma^*$

$$A\mathbf{x} = \omega B\mathbf{x} \longrightarrow \widehat{A}_r \mathbf{y}_r = \omega \left(\imath \begin{bmatrix} 0 & \Sigma_r^{-1} \\ -\Sigma_r^{-1} & 0 \end{bmatrix} \right) \mathbf{y}_r \equiv \omega \widehat{B}_r \mathbf{y}_r,$$

$\widehat{B}_r$ is Hermitian and indefinite

and

$$\begin{bmatrix} \mathbf{h}^\top & \mathbf{e}^\top \end{bmatrix}^\top = \imath \begin{bmatrix} -I_{3n} & -\zeta_d \\ \xi_d & \varepsilon_d \end{bmatrix}^{-1} \mathrm{diag}\left(P_r, Q_r\right) \mathbf{y}_r,$$

where

$$\widehat{A}_r := \widehat{A}_r(\gamma) \equiv \mathrm{diag}(P_r^*, Q_r^*) \begin{bmatrix} \zeta_d & -I_{3n} \\ I_{3n} & 0 \end{bmatrix} \begin{bmatrix} \Phi^{-1} & 0 \\ 0 & I_{3n} \end{bmatrix} \begin{bmatrix} \xi_d & I_{3n} \\ -I_{3n} & 0 \end{bmatrix} \mathrm{diag}(P_r, Q_r)$$

with $\Phi := \Phi(\gamma) \equiv \varepsilon_d - \xi_d \zeta_d$ being Hermitian.

- when $\gamma < \gamma^*$, $\widehat{A}_r$ is Hermitian and positive definite, then $(\widehat{A}_r, \widehat{B}_r)$ has all eigenvalues being positive real } **(FAST!!!)** **inverse Lanczos method**

- when $\gamma > \gamma^*$, $\widehat{A}_r$ is Hermitian and indefinite, then $(\widehat{A}_r, \widehat{B}_r)$ is indefinite and has complex eigenvalues } **shift-and-inverse Arnoldi method**

Chiral media (3D)

Consider the FCC lattice with chiral media. The radius r of the spheres and the minor axis length s of the spheroids are $r = 0.08a$ and $s = 0.06a$ with a being the lattice constant. Take the relative permittivity $\varepsilon_i = 13$ and then $\gamma^* = \sqrt{13} \approx 3.606$.

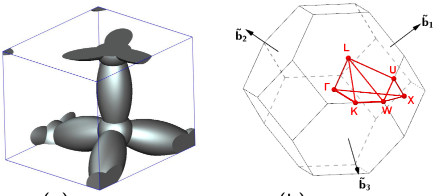

(a) physical cell (b) working cell

Figure: Illustration of the 3D physical cell and Brillouin zone of the FCC lattice

- The mesh numbers $n_1 = n_2 = n_3 = 96$ and the matrix dimension of $\widehat{A}_r$ is 3,538,944. Furthermore, the stopping tolerance is set to be 10^{-12}.

Anticrossing eigencurves

The influence of the resonance modes for band structures.

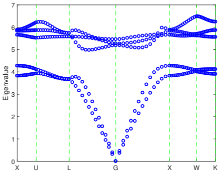

(a) $\gamma = 3.607$

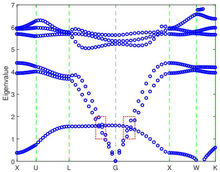

(b) $\gamma = 3.61302$

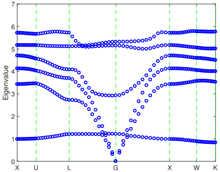

(c) $\gamma = 3.6138$

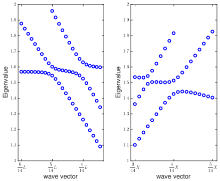

(d) Zoom-in at $\gamma = 3.61302$

Figure: Band structures.

Condensations of eigenvectors with $\gamma = 1 < \gamma^*$

In the following, we study the relationship between the condensation and the parameter γ.

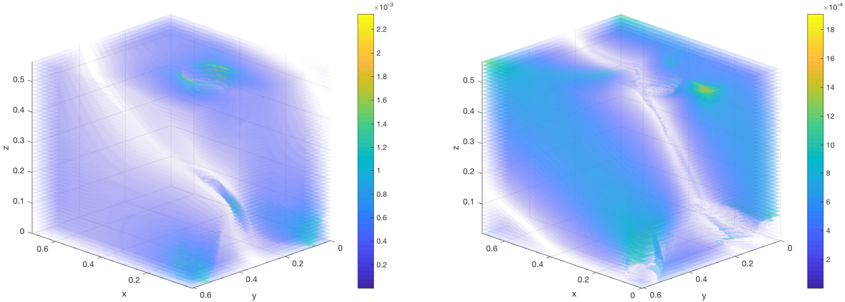

(a) $(\lambda_1, \mathbf{e}_1)$ (b) $(\lambda_3, \mathbf{e}_3)$

Figure: The absolute values of the first and third eigenmodes for $\mathbf{e}_1$ and $\mathbf{e}_3$ with $\gamma = 1$.

Condensations of eigenvectors with $\gamma > \gamma^*$

- The absolute values of $\mathbf{e}_2$ corresponding to the first smallest positive eigenvalue (resonance mode) with $\mathbf{k} = \frac{6}{14}L$ are shown.
- In order to measure the neighborhood, we define new radius of the sphere and the connecting spheroid to be ρr and ρs, respectively.

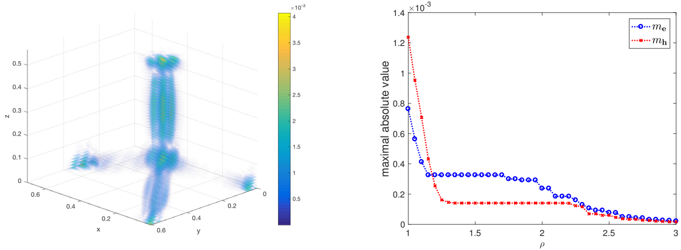

(a) $|\mathbf{e}_2|$ (b) $m_{\mathbf{e}}$ and $m_{\mathbf{h}}$

Figure: The absolute values of $\mathbf{e}_2$, $m_{\mathbf{e}}$, $m_{\mathbf{h}}$ for the resonance mode.

Condensations of eigenvectors

According to the mesh indices belonging to the material or not, we separate $\mathbf{e}$ and $\mathbf{h}$ as $(\mathbf{e}_i, \mathbf{e}_o)$ and $(\mathbf{h}_i, \mathbf{h}_o)$, where the index i/o denotes inside/outside the material. Since $\mathbf{e}^*\mathbf{e} + \mathbf{h}^*\mathbf{h} = 1$, we use the ratios $\frac{\mathbf{e}_o^*\mathbf{e}_o}{\mathbf{e}_i^*\mathbf{e}_i}$ and $\frac{\mathbf{h}_o^*\mathbf{h}_o}{\mathbf{h}_i^*\mathbf{h}_i}$ to determine the condensations of the electric and magnetic fields. The results in Figure 3.6 show that these ratios are decreasing as γ increases.

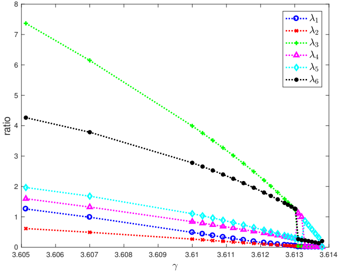

(a) $\frac{\mathbf{e}_o^*\mathbf{e}_o}{\mathbf{e}_i^*\mathbf{e}_i}$

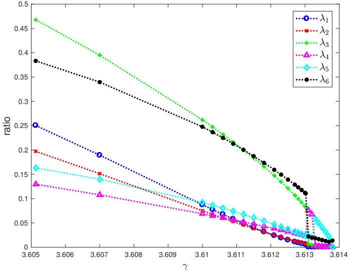

(b) $\frac{\mathbf{h}_o^*\mathbf{h}_o}{\mathbf{h}_i^*\mathbf{h}_i}$

Figure: Ratios $\frac{\mathbf{e}_o^*\mathbf{e}_o}{\mathbf{e}_i^*\mathbf{e}_i}$ and $\frac{\mathbf{h}_o^*\mathbf{h}_o}{\mathbf{h}_i^*\mathbf{h}_i}$ for the six smallest positive eigenvalues vs. various γ.

Fast Algorithm for Maxwell's Equations

http://www.njcam.org.cn/fame/index.phtml

FAME

Fast Algorithms for Maxwell Equations

Home Background BandStructure Publications Downloads Team

Fast Algorithms for Maxwell's Equations (FAME) is a package for solving three-dimensional source-free Maxwell's equations with periodical structures

High-performance Implementations

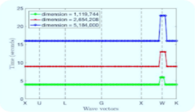

Ultrafast Parallelizations on Multi-GPU

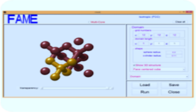

User Friendly GUI in MATLAB

Breakthrough Mathematical Algorithms

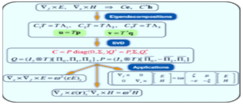

Singular Value Decomposition

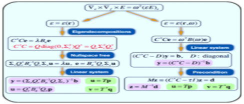

Null-space Free Eigensolver

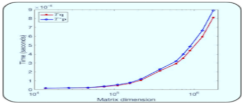

Fast FFT-based Matrix Vector Multiplications

Maximum Versatility for All 14 Bravais Lattices

Downloads

编辑: 来源: 时间: 2021-04-09 点击: 39

FAME on GPU FAME on MATLAB

扫描二维码
将文章分享给好友

产品更新 | Ubuntu版进入3.0时代， 北太天元FAME插件重磅首发！

北太振寰 2023-12-01 11:00 发表于重庆

收录于合集
#产品更新
8个 >

北太天元（Ubuntu版）*已更新至v3.0！

“不止于3.0”

Ubuntu版FAME插件重磅首发！

与北太天元（Windows版）v3.0相比，Ubuntu 版已上线FAME插件， 插件由**南京应用数学中心林文伟教授和东南大学李铁香教授团队**设计研发。

01

走近FAME：

三维光子晶体能带结构计算的快速算法

光子晶体是由不同折射率的介质周期性排列而形成的规则结构材料， 具有普通光学材料所不具备的光子禁带特性， 在科学界和产业界被称为“光半导体”或“未来的半导体”， 被誉为**二十一世纪最具潜力的新型材料**。

Contents

Conclusions

1. For the Maxwell eigenvalue problems arising in 3D anisotropic photonic crystals, we want to calculate some smallest positive eigenvalues.
2. The explicit SVD of the discrete curl matrix $\mathcal{C}$ arising from Yee's FD in the oblique coordinate systems is constructed.
3. A null-space free technique to deflate the null space of the large-scale GEP and then an eigensolver called "FAME" based on 3D FFT are developed.
4. The special eigenvalue behaviors and condensation of eigenvectors of the 3D chiral photonic crystals are found theoretically and numerically.
5. In the furthermore work, these techniques can be generalized and applied to phononic crystals, photonic quasi-crystals, and to discover more physical phenomena ......

Thanks for your attention!